PERGAMON

Chemical Engineering Science 55 (2000) 2923–2930

Chemical Engineering Science

The generalized Maxwell–Stefan model for diffusion in zeolites: sorbate molecules with different saturation loadings

F. Kapteijn[a,*], J. A. Moulijn[a], R. Krishna[b]

[a]*Chemical Engineering Department, Industrial Catalysis, Delft University of Technology, Julianalaan 136, 2628 BL Delft, Netherlands*
[b]*Department of Chemical Engineering, University of Amsterdam, Nieuwe Achtergracht 166, 1018 WV Amsterdam, Netherlands*

Received 3 June 1999; received in revised form 23 September 1999; accepted 9 November 1999

Abstract

Using the Maxwell–Stefan approach, expressions have been derived for the diffusion of mixtures of hydrocarbons in zeolites wherein the individual components have different saturation loadings. This Maxwell–Stefan diffusion model, in combination with the Ideal Adsorbed Solution (IAS) theory and the single-component adsorption isotherms, provides a superior, qualitative and quantitative, prediction of the permeation fluxes of ethane/methane and propane/methane mixtures through a silicalite-1 membrane. The difference in adsorption saturation loadings becomes apparent in the entropy effects in the mixture adsorption.

Keywords: Zeolite diffusion; Maxwell–Stefan theory; Ideal adsorption solution (IAS); Saturation loading; Membrane permeation

1. Introduction

The Generalized Maxwell–Stefan (GMS) equations have successfully been applied to many systems to describe diffusive transport phenomena in multicomponent mixtures (Krishna & Wesselingh, 1997). The GMS model is based on the principle that in order to cause relative motion between individual species in a mixture, a driving force has to be exerted on each of the individual species. The driving force exerted on any particular species i is balanced by the friction this species experiences with all other species present in the mixture. Each of these friction contributions is considered to be proportional to the corresponding differences in the diffusion velocities. Diffusion in porous solid materials, relevant in adsorption, catalysis and separation processes, is incorporated in the formulations (Krishna, 1993b).

Krishna (1990,1993a,b) extended this approach to describe the surface diffusion of adsorbed molecules, starting from Eq. (1) for an n-component mixture.

$$-\nabla\mu_i = RT\sum_{\substack{j=1\\ j\neq i}}^{n}\theta_j\frac{u_i-u_j}{Đ_{ij}^s} + RT\frac{u_i}{Đ_i^s},\quad i=1,2,\ldots n \qquad (1)$$

where $-\nabla\mu_i$ is the force acting on species i tending to move along the surface with a velocity u_i. The first term on the right-hand side reflects the friction exerted by adsorbate j on the surface motion of species i, each moving with velocities u_j and u_i with respect to the surface, respectively. The second term reflects the friction between the species i and the surface. $Đ_{ij}^s$ and $Đ_i^s$ represent the corresponding Maxwell–Stefan surface diffusivities. The $Đ_i^s$ is also called the corrected diffusivity in the literature; cf. Ruthven (1984). The fractional surface occupancies are given by θ_j.

The GMS formulation (1) has been applied successfully to describe transient uptake in zeolites and carbon molecular sieves, and in zeolitic membrane permeation (Van de Graaf, Kapteijn & Moulijn, 1999). Generally, a multicomponent Langmuir-type adsorption model is used to describe the fractional occupancies. For thermodynamic consistency, however, the saturation loading for all species must be equal in the multicomponent Langmuir model (Sircar, 1991), hence we define the fractional occupancies as

$$\theta_i = \frac{q_i}{q^{\text{sat}}}. \qquad (2)$$

Recently, much work has been done on the single-component adsorption on MFI-type zeolites, silicalite-1 and ZSM-5, both experimental (Guo, Talu & Hayhurst, 1989;

* Corresponding author. Fax: 00-31-15-278-4452.
E-mail address: f.kapteijn@tnw.tudelft.nl (F. Kapteijn)

0009-2509/00/$ - see front matter
PII: S0009-2509(99)00564-3

Nomenclature

B_{ij}	elements of matrix $[B]$, defined in Eq. (13), s/m^2
B'_{ij}	elements of matrix $[B']$, defined in Eq. (12)
$Đ_i$	Maxwell-Stefan zeolite diffusivity for species i, m^2/s
$Đ_{ij}$	Maxwell-Stefan diffusivity describing interchange between i and j, m^2/s
K_A	adsorption coefficient for site A, Pa^{-1}
K_B	adsorption coefficient for site B, Pa^{-1}
n	number of components in the mixture
N_i	molecular flux of species i, molecules/m^2/s or mol/m^2/s
p_i	partial pressure of species i, Pa
q_i	loading of component i in zeolite, molecules per unit cell or mol/kg
R	gas constant, 8.314 J/mol/K
T	temperature, K
u_i	velocity of species i with respect to zeolite, m/s

Greek letters

Γ_{ij}	elements of matrix of thermodynamic correction factor, $[\Gamma]$, dimensionless
∇	gradient operator, m^{-1}
θ_i	fractional loading of component i, dimensionless
μ	chemical potential, J/mol
ρ	density of membrane, number of unit cells per m^3 or kg/m^3

Subscripts

A	referring to site A
B	referring to site B
1	component 1 in binary mixture
2	component 2 in binary mixture

Superscripts

s	referring to surface diffusion
sat	referring to saturation loading

Sun, Talu & Shah, 1996; Sun, Shah, Xu & Talu, 1996; Takaishi, Tsutsumi, Chubuchi & Matsumoto, 1998; Song & Rees, 1997; Zhu, Graaf, Broeke, Kapteijn & Moulijn, 1998) and molecular simulations (Vlugt, Krishna & Smit, 1999; Du, Manos, Vlugt & Smit, 1998; Smit, 1995; Smit & Maesen, 1995). In the MFI structure straight channels are connected via zig-zag channels, which forms a pore network, where different adsorption locations can be distinguished. Generally speaking one distinguishes between two distinct sorption sites: within the channel interiors and at the intersections of the straight and zig-zag channels (Ashtekar, Hastings & Gladden, 1998).

Single-component adsorption of linear and branched hydrocarbons in MFI-type zeolites can be well described by single- or dual-site Langmuir models, Eq. (3) (Micke, Bülow, Kocirik & Struve, 1994; Song & Rees, 1997; Zhu et al., 1998), where the different sites A and B may be represented by channel interiors and the intersections.

$$q_i = q_{iA}^{\text{sat}} \frac{K_{iA} p_i}{1 + K_{iA} p_i} + q_{iB}^{\text{sat}} \frac{K_{iB} p_i}{1 + K_{iB} p_i}, \tag{3}$$

$$q_i^{\text{sat}} = q_{iA}^{\text{sat}} + q_{iB}^{\text{sat}}. \tag{4}$$

Configurational-Bias Monte-Carlo (CBMC) simulations nicely demonstrate not only the adsorption isotherm behaviour but also the siting of the molecules, in agreement with the classification into channels and intersections (Vlugt, Zhu, Kapteijn, Moulijn, Smit & Krishna, 1998; Vlugt et al., 1999). The total saturation loading q_i^{sat} of the various molecules, Eq. (4), may differ significantly. For alkanes q_i^{sat} depends on the chain length and the degree of branching (Fig. 1). Linear alkanes occupy both channel and intersection space, while branched molecules prefer to reside at the intersections (Vlugt et al., 1999). Singly branched molecules may partly occupy the channel space, while double-branched molecules only occupy the intersections (Vlugt et al., 1999). The adsorption isotherm shows an inflection corresponding with the point where the first type of site becomes saturated, reflecting the step-wise filling of the different types of sites (Krishna, Smit & Vlugt, 1999). Similar trends have been observed for aromatic molecules (Guo et al., 1989; Shah, Guo & Hazhurst, 1995; Rudzinski, Narkierwiez-Michalek, Szabelski & Chiang, 1997).

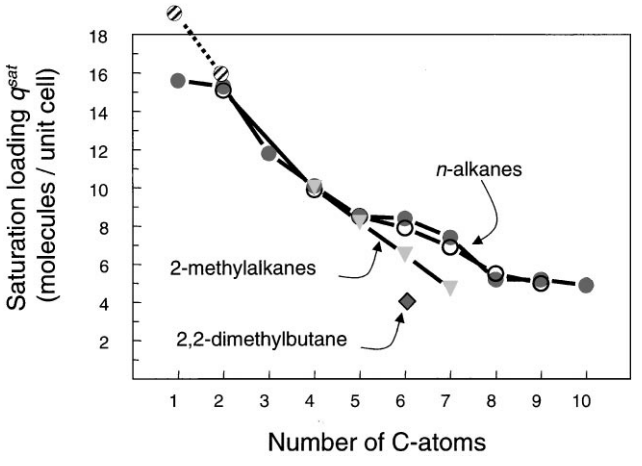

Fig. 1. Saturation loadings (molecules per unit cell) of alkanes in silicalite-1: (▨) experimental data of Sun et al. (1996) and Sun et al. (1998) ; (●,▽,◆) CBMC data from Vlugt et al. (1999) and Du et al. (1998). Vlugt recalculated a higher saturation loading for methane than in the Du et al., paper.

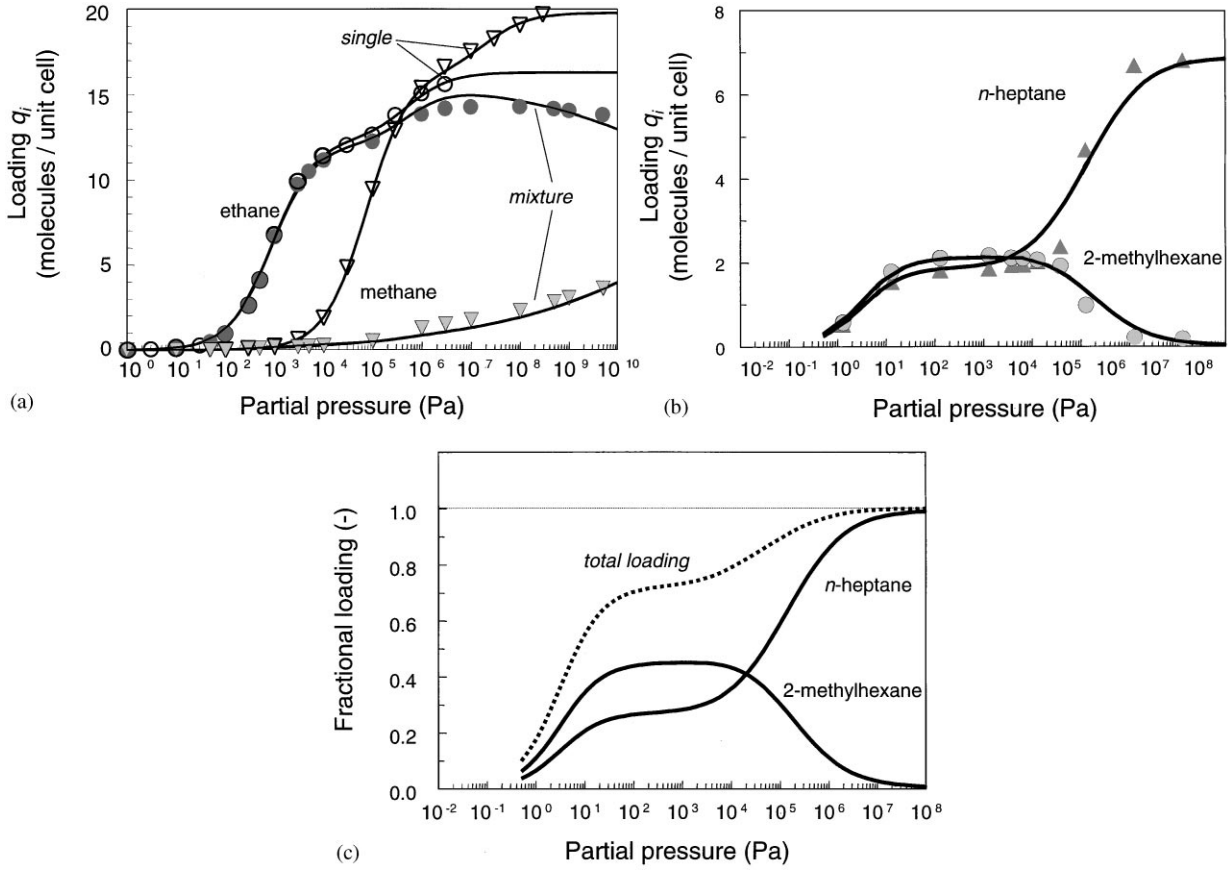

Fig. 2. Comparison of the binary adsorption of methane and ethane and of n-heptane and 2-methylhexane in silicalite-1 obtained by CBMC simulation (Du et al., 1998; Krishna et al., 1998) and calculated by application of IAS theory using the dual-site Langmuir model for the individual components: (a) methane (▽,▽) — ethane (●,○) system at 250 K. Open symbols single components with lines a dual site Langmuir fit, solid symbols equimolar mixture with lines IAS prediction; Isotherm parameters: methane $q_A^{sat} = 16.3$ molec./u.c., $K_A = 1.33 \times 10^{-5}$ Pa^{-1}, $q_B^{sat} = 3.4$ molec./u.c., $K_B = 4.81 \times 10^{-8}$ Pa^{-1}; ethane $q_A^{sat} = 12.3$ molec./u.c., $K_A = 1.124 \times 10^{-3}$ Pa^{-1}, $q_B^{sat} = 3.9$ molec./u.c., $K_B = 1.88 \times 10^{-6}$ Pa^{-1}; (b) n-heptane (▲) and 2-methylhexane (●) equimolar mixture at 374 K with loading in molecules per unit cell (molec./u.c.); (c) same mixture, fractional loading as a function of the partial pressure. Isotherm parameters: n-heptane $q_A^{sat} = 4.0$ molec./u.c., $K_A = 0.15$ Pa^{-1}, $q_B^{sat} = 2.9$ molec./u.c., $K_B = 3 \times 10^{-5}$ Pa^{-1}; 2-methylhexane $q_A^{sat} = 4.0$ molec./u.c., $K_A = 0.17$ Pa^{-1}, $q_B^{sat} = 0.7$ molec./u.c., $K_B = 2 \times 10^{-9}$ Pa^{-1}.

The different saturation loadings for the different molecules preclude the application of the multicomponent Langmuir isotherm for mixtures and, hence, the application to the GMS equations derived for this condition (Krishna, 1993b; Krishna et al., 1999).

The objective of this communication is to present an extension of the multi-component diffusion equations for the case depicted above, where individual molecules have different saturation loadings.

2. The Maxwell–Stefan theory for zeolite diffusion

To develop expressions for the diffusional fluxes from Eq. (1), the driving force, the gradient of the thermodynamic potential of a component is related to gradient in loading through the partial pressure and the mixture adsorption isotherm. The fractional occupancies are converted into fluxes using Eq. (5).

$$N_i \equiv \rho q_i^{sat} \theta_i u_i = \rho q_i u_i \tag{5}$$

which includes the definition of fractional occupancy by

$$\theta_i = \frac{q_i}{q_i^{sat}}. \tag{6}$$

This implies that for different molecules different amounts are needed to obtain similar levels of fractional occupancies. For di-branched molecules saturation is reached at lower loadings than for linear ones, since their packing is less efficient. This results in a situation that at high pressures molecules with the largest saturation loading will be preferentially adsorbed for entropic reasons, i.e. the largest number of molecules are filling the pore space. This is theoretically demonstrated for mixture adsorption of hard rods of different size (Bakaev & Steele, 1997) and through CBMC simulations for binary mixture adsorption of linear and branched alkanes in silicalite-1 (Du et al., 1998; Krishna, Smit & Vlugt, 1998; Vlugt et al., 1999). Examples are given in Fig. 2a for a mixture of methane and ethane and in Fig. 2b for an

n-heptane and 2-methylhexane mixture. For the methane–ethane mixture the stronger adsorbing component is preferentially adsorbed but at higher pressures the higher saturation capacity of methane becomes important. The methane loading gradually increases while the ethane loading passes through a maximum with increasing pressure. For the n-heptane and 2-methylhexane mixture the effect of a packing efficiency difference is more pronounced. High, entropy controlled, adsorption selectivities may be achieved at elevated pressures for mixtures of branched and linear alkanes.

Essential for the further development is a thermodynamically consistent model for the mixture adsorption. Various approaches have been proposed for mixtures (e.g. Myers & Prausnitz, 1965; Sircar, 1991; Sircar, 1995; Maurer, 1997). Here the ideal adsorbed solution (IAS) theory of Myers and Prausnitz (1965) will be used, which is thermodynamically consistent and can be applied by using the single-component isotherms. The other models referred to are not able to describe the inflection behaviour of the single-component isotherms. The IAS approach requires the numerical solution of a set of equations, which can be performed efficiently by the iterative 'fast-IAS' approach, outlined by O'Brien and Myers (1988). The correspondence of the IAS calculations with the CBMC simulations (Du et al., 1998; Krishna et al., 1998), given in Figs. 2a and b is excellent. The used adsorption parameters of the single-component isotherms for methane, ethane, n-heptane and 2-methylhexane were determined by nonlinear regression from the single-component CBMC data on the dual-site Langmuir model. These were used as input for the IAS calculations. Recently, Macedonia and Maginn (1999) showed the good correspondence of IAS and grand canonical Monte Carlo simulations for lower alkane mixtures, while Dunne, Rao, Sircar, Gorte & Myers (1997) showed this for experimental data on methane–ethane, although for lower pressures. Of course, at higher pressures the ideality of the mixture will not be valid any more and deviations may be observed, the current approach must be considered as a good first approximation.

The definition of the fractional loading is illustrated in Fig. 2c for the data of Fig. 2b. The lower saturation loading of 2-methylhexane results in a higher fractional loading in the pressure region of the inflection, where the absolute loadings (molec./u.c.) of both components are about equal. The total fractional occupancy evolves with increasing pressure to one, as is required by definition.

Dropping the superscripts for the surface diffusivities in the GMS expression for convenience, multiplication of both sides by θ_i/RT and application of Eq. (6), Eq. (1) can be recast into

$$-\frac{\theta_i}{RT}\nabla\mu_i = \sum_{\substack{j=1\\ j\neq i}}^{n} \theta_i\theta_j \frac{u_i - u_j}{Đ_{ij}} + \frac{\theta_i u_i}{Đ_i}$$

$$= \sum_{\substack{j=1\\ j\neq i}}^{n} q_i q_j \frac{u_i - u_j}{q_i^{sat} q_j^{sat} Đ_{ij}} + \frac{q_i u_i}{q_i^{sat} Đ_i}, \quad i = 1, 2, \ldots n. \tag{7}$$

Using the definition of the fluxes, Eq. (5), leads to

$$-\rho\frac{\theta_i}{RT}\nabla\mu_i = \sum_{\substack{j=1\\ j\neq i}}^{n} \frac{q_j N_i - q_i N_j}{q_i^{sat} q_j^{sat} Đ_{ij}} + \frac{N_i}{q_i^{sat} Đ_i}, \quad i = 1, 2, \ldots n. \tag{8}$$

The gradient of the thermodynamic potential can be expressed in terms of thermodynamic factors (Krishna, 1993b)

$$\frac{\theta_i}{RT}\nabla\mu_i = \sum_{j=1}^{n} \Gamma_{ij}\nabla\theta_j, \quad \Gamma_{ij} \equiv \frac{\theta_i}{p_i}\frac{\partial p_i}{\partial\theta_j}, \quad i, j = 1, n. \tag{9}$$

It is noted that for calculation convenience in using the IAS theory, the thermodynamic factors may be expressed in absolute loadings (e.g. mol/kg or molecules per unit cell) by

$$\Gamma_{ij} \equiv \left(\frac{q_j^{sat}}{q_i^{sat}}\right)\frac{q_i}{p_i}\frac{\partial p_i}{\partial q_j}, \quad i, j = 1, n. \tag{10}$$

This includes the ratio of the saturation loadings of i and j, which is unequal one for $i \neq j$, i.e. for the off-diagonal terms.

Eq. (8) and Eq. (9) can be cast into a matrix–vector notation:

$$-\rho[\Gamma](\nabla\theta) = [B'](N) = [B][q^{sat}]^{-1}(N), \tag{11}$$

where $[q^{sat}]$ is a diagonal matrix of saturation loadings and the elements of $[B']$ and $[B]$ are given by the following equations

$$B'_{ii} = \frac{1}{q_i^{sat} Đ_i} + \sum_{\substack{j=1\\ j\neq i}}^{n} \frac{q_j}{q_i^{sat} q_j^{sat} Đ_{ij}},$$

$$B'_{ij} = -\frac{q_i}{q_i^{sat} q_j^{sat} Đ_{ij}}, \quad i \neq j \tag{12}$$

and

$$B_{ii} = \frac{1}{Đ_i} + \sum_{\substack{j=1\\ j\neq i}}^{n} \frac{\theta_j}{Đ_{ij}},$$

$$B_{ij} = -\frac{\theta_i}{Đ_{ij}}, \quad i \neq j. \tag{13}$$

The solution of Eq. (11) for the fluxes is given by

$$(N) = -\rho[B']^{-1}[\Gamma](\nabla\theta) = -\rho[q^{sat}][B]^{-1}[\Gamma](\nabla\theta). \tag{14}$$

This result differs from the original formulation of Krishna (1993b) by the presence of the diagonal matrix of saturation loadings $[q_{sat}]$. Note also the scaling of the off-diagonal terms in the $[\Gamma]$ matrix by the ratio of the corresponding saturation loadings, if the elements of this matrix are calculated from the absolute loadings, cf. Eq. (10).

3. Two-component system expressions — application to membrane permeation

For a two-component system, which is most often used experimentally, the mathematical treatment is outlined more extensively below. The matrices are

$$[\Gamma] = \begin{bmatrix} \Gamma_{11} & \Gamma_{12} \\ \Gamma_{21} & \Gamma_{22} \end{bmatrix}, \tag{15}$$

$$[B'] = \begin{bmatrix} \dfrac{1}{q_1^{sat}Đ_1} + \dfrac{q_2}{q_1^{sat}q_2^{sat}Đ_{12}} & -\dfrac{q_1}{q_1^{sat}q_2^{sat}Đ_{12}} \\ -\dfrac{q_2}{q_1^{sat}q_2^{sat}Đ_{12}} & \dfrac{1}{q_2^{sat}Đ_2} + \dfrac{q_1}{q_1^{sat}q_2^{sat}Đ_{12}} \end{bmatrix} = \begin{bmatrix} \dfrac{1}{Đ_1} + \dfrac{\theta_2}{Đ_{12}} & -\dfrac{\theta_1}{Đ_{12}} \\ -\dfrac{\theta_2}{Đ_{12}} & \dfrac{1}{Đ_2} + \dfrac{\theta_1}{Đ_{12}} \end{bmatrix} \begin{bmatrix} \dfrac{1}{q_1^{sat}} & 0 \\ 0 & \dfrac{1}{q_2^{sat}} \end{bmatrix} = [B][q^{sat}]^{-1}, \tag{16}$$

$$[B']^{-1} = \begin{bmatrix} q_1^{sat} & 0 \\ 0 & q_2^{sat} \end{bmatrix} \frac{\begin{bmatrix} \left(\dfrac{1}{Đ_2} + \dfrac{\theta_1}{Đ_{12}}\right) & \dfrac{\theta_1}{Đ_{12}} \\ \dfrac{\theta_2}{Đ_{12}} & \left(\dfrac{1}{Đ_1} + \dfrac{\theta_2}{Đ_{12}}\right) \end{bmatrix}}{\dfrac{\theta_1}{Đ_1Đ_{12}} + \dfrac{\theta_2}{Đ_2Đ_{12}} + \dfrac{1}{Đ_1Đ_2}} = [q^{sat}][B]^{-1} \tag{17}$$

and the inverted B-matrix can be written as

$$[B]^{-1} = \begin{bmatrix} Đ_1 & 0 \\ 0 & Đ_2 \end{bmatrix} \begin{bmatrix} \left(1 + \theta_1\dfrac{Đ_2}{Đ_{12}}\right) & \theta_1\dfrac{Đ_2}{Đ_{12}} \\ \theta_2\dfrac{Đ_1}{Đ_{12}} & \left(1 + \theta_2\dfrac{Đ_1}{Đ_{12}}\right) \end{bmatrix} \frac{1}{1 + \theta_1\dfrac{Đ_2}{Đ_{12}} + \theta_2\dfrac{Đ_1}{Đ_{12}}}. \tag{18}$$

Substitution of Eqs. (15)–(18) into Eq. (14) yields for the fluxes

$$N_1 = -\rho \frac{q_1^{sat}Đ_1\left[\left\{\Gamma_{11} + \theta_1\dfrac{Đ_2}{Đ_{12}}(\Gamma_{11} + \Gamma_{21})\right\}\nabla\theta_1 + \left\{\Gamma_{12} + \theta_1\dfrac{Đ_2}{Đ_{12}}(\Gamma_{12} + \Gamma_{22})\right\}\nabla\theta_2\right]}{\theta_2\dfrac{Đ_1}{Đ_{12}} + \theta_1\dfrac{Đ_2}{Đ_{12}} + 1}, \tag{19a}$$

$$N_2 = -\rho \frac{q_2^{sat}Đ_2\left[\left\{\Gamma_{22} + \theta_2\dfrac{Đ_1}{Đ_{12}}(\Gamma_{22} + \Gamma_{12})\right\}\nabla\theta_2 + \left\{\Gamma_{21} + \theta_2\dfrac{Đ_1}{Đ_{12}}(\Gamma_{21} + \Gamma_{11})\right\}\nabla\theta_1\right]}{\theta_2\dfrac{Đ_1}{Đ_{12}} + \theta_1\dfrac{Đ_2}{Đ_{12}} + 1}. \tag{19b}$$

Alternatively, if gradients are expressed in absolute loadings, like mol/kg, the expressions become

$$N_1 = -\rho \frac{Đ_1\left[\left\{\Gamma_{11} + \theta_1\dfrac{Đ_2}{Đ_{12}}(\Gamma_{11} + \Gamma_{21})\right\}\nabla q_1 + \left\{\Gamma_{12} + \theta_1\dfrac{Đ_2}{Đ_{12}}(\Gamma_{12} + \Gamma_{22})\right\}\left(\dfrac{q_1^{sat}}{q_2^{sat}}\right)\nabla q_2\right]}{\theta_2\dfrac{Đ_1}{Đ_{12}} + \theta_1\dfrac{Đ_2}{Đ_{12}} + 1}, \tag{20a}$$

$$N_2 = -\rho \frac{Đ_2\left[\left\{\Gamma_{22} + \theta_2\dfrac{Đ_1}{Đ_{12}}(\Gamma_{22} + \Gamma_{12})\right\}\nabla q_2 + \left\{\Gamma_{21} + \theta_2\dfrac{Đ_1}{Đ_{12}}(\Gamma_{21} + \Gamma_{11})\right\}\left(\dfrac{q_2^{sat}}{q_1^{sat}}\right)\nabla q_1\right]}{\theta_2\dfrac{Đ_1}{Đ_{12}} + \theta_1\dfrac{Đ_2}{Đ_{12}} + 1}. \tag{20b}$$

Table 1
Parameter values used in the membrane permeation modeling for 303 K (Van de Graaf et al., 1999; Zhu et al., 1998)

		q_i^{sat} (mol/kg)	K_i (10^{-6} Pa^{-1})	$Đ_i$ (10^{-10} m^2 s^{-1})
Methane		2.24	2.20	10.4
Ethane		1.85	56.7	1.50
Propane		1.58	650	0.34
Methane[a]	(In mixture with ethane)	1.85	3.1	
	(In mixture with propane)	1.58	4.0	

[a]These parameters were used in the extended Langmuir expression for mixtures to ensure thermodynamic consistency.

This result is nearly identical to that for an approach where one saturation concentration is used, except for the presence of the different saturation capacities as multiplier in Eq. (19a) and (19b), or, if real loading gradients are used in Eq. (20a) and (20b), the use of a kind of scaling factor, the ratio of the saturation capacities of the components under consideration. The latter can be rationalised if one realizes that the absolute loading gradients depend on these saturation capacities. To convert the gradient of one component into that of the other one needs this ratio to scale the interconversion.

The present result is consistent with the case that the saturation capacities are equal, the diagonal matrix of the saturation capacities becomes a scalar and (14) reduces to the original two-component expression. Another simplification that has been applied to the 'full' GMS model above, is the assumption that there is no interaction between the components, i.e. the terms with the $Đ_{ij}$ vanish (numerically $Đ_{ij} \to \infty$). Matrix $[B]^{-1}$ then reduces to a simple diagonal matrix of the single-component's Maxwell–Stefan diffusivities

$$[B]^{-1} = \begin{bmatrix} Đ_1 & 0 \\ 0 & Đ_2 \end{bmatrix} \tag{21}$$

and the flux expression (20a) for component 1 becomes

$$\begin{aligned} N_1 &= -\rho Đ_1 \left[\Gamma_{11} \nabla q_1 + \Gamma_{12} \left(\frac{q_1^{sat}}{q_2^{sat}} \right) \nabla q_2 \right] \\ &= -\rho Đ_1 \left[\left(\frac{q_1}{p_1} \frac{\partial p_1}{\partial q_1} \right) \nabla q_1 + \left(\frac{q_1}{p_1} \frac{\partial p_1}{\partial q_2} \right) \nabla q_2 \right] \end{aligned} \tag{22}$$

in which the definition of the thermodynamic factor, Eq. (10), has been substituted. For this particular case the factor of the ratio of the saturation loadings has disappeared (cf. Eq. (20a)), although the different saturation loadings are still present in the mixture adsorption model. Van den Broeke, Bakker, Kapteijn and Moulijn (1999) applied this model in combination with IAS for weakly adsorbing gases.

As an example the outlined expressions have been applied to the prediction of selectivities in the binary permeation of methane/ethane and methane/propane mixtures through a silicalite-1 membrane, components of which the saturation loadings are different (Van de Graaf et al., 1999). The original parameters for the adsorption were taken from Zhu et al. (1998), which had been used to determine the Maxwell–Stefan diffusivity values on the basis of unary permeation measurements. To remain thermodynamically consistent and to apply the extended single-site Langmuir isotherm in the mixture permeation simulations, Van de Graaf et al. (1999) re-estimated the methane adsorption parameters from the single-component methane adsorption data by fixing the methane saturation loading to that of the other component in their calculation. The parameter values used for the calculations are given in Table 1. For the calculation of the $Đ_{ij}$ the Vignes correlation as proposed by Krishna (1993b) was employed.

$$Đ_{12} = Đ_1^{\theta_1/(\theta_1+\theta_2)} Đ_2^{\theta_2/(\theta_1+\theta_2)}. \tag{23}$$

Figs. 3a and b represent the simulations based on the IAS approach outlined above for ethane/methane and propane/methane, respectively. Included further are the original experimental data and the extended Langmuir isotherm simulations with equal saturation loadings for either component. The total hydrocarbon permeate pressure was kept fixed at 20 and 10 kPa, respectively, to approach the experimental conditions, since these finite permeate pressures have a considerable influence (Van de Graaf, Van der Bijl, Stol, Kapteijn & Moulijn, 1998). These two examples were selected since the single-site Langmuir approach gave the largest deviation for the selectivity. In both cases the experimental data exhibit a declining tendency for the selectivity, while the Langmuir model evolves to a limiting value. It is noted here that an IAS calculation with the equal saturation loadings is the same as the extended Langmuir model. The IAS approach with the different saturation loadings is clearly able to predict the decreasing trends of the experimental data in both figures. For the 1 : 1 ethane/methane mixture the increasing total pressure is relatively more favourable for the methane adsorption, see Fig. 2a, and the ethane selectivity decreases. In the propane/methane

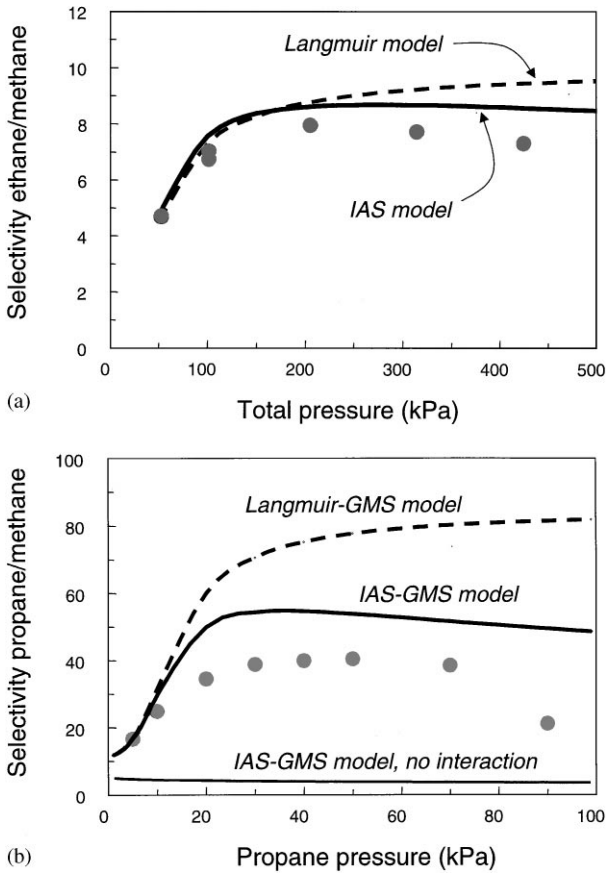

Fig. 3. Comparison of selectivities for binary mixture permeation through a silicalite-1 membrane; (a) ethane/methane equimolar feed mixture at 303 K as a function of the total feed pressure, permeate pressure 20 kPa; (b) propane/methane mixture at 303 K and 100 kPa total feed pressure as a function of the propane pressure, permeate pressure 10 kPa. Key: (●) experimental data Van de Graaf et al. (1999); dashed curves Langmuir based model (equal saturation loadings); solid curves IAS-based GMS model, Eq. (20a) and (20b). In Fig. 3b is included the GMS model without interaction term, Eq. (22).

mixture a similar reason holds for the variation in composition. So, these subtle details in the permeation selectivities only become apparent if the different values of the saturation loadings are taken into consideration in the mixture adsorption, and, consequently, in the diffusion equations. The model without the $Đ_{ij}$ interaction terms is not capable of predicting the results for propane/methane. Analysis of various simulation results revealed that

(i) For mixtures of components with quite different diffusivity values the presence of $Đ_{ij}$ is necessary. If the differences are small then the influence of this term is negligible, which was about the case for the results of Van den Broeke et al. (1999).

(ii) The mixture adsorption at the feed (= retentate) side determines to a large extent the separation performance. So a good mixture adsorption model that accounts for the differences in saturation loadings in combination with the GMS relations will perform superior to other models for permeation predictions.

4. Conclusions

On the basis of the Maxwell–Stefan approach expressions have been derived for the description of mixture diffusion in zeolites of hydrocarbons with different saturation loadings. In combination with the IAS theory, that can handle the mixture adsorption for this case, a superior qualitative and quantitative prediction is obtained for the mixture permeation of ethane/methane and propane/methane through a silicalite-1 membrane, using only the single-component parameter values. The difference in adsorption saturation loadings becomes apparent in the entropy effects in the mixture adsorption.

Acknowledgements

The authors acknowledge Thijs Vlugt for providing the unary CBMC adsorption calculations for methane and ethane in Fig. 2a.

References

Ashtekar, S., Hastings, J. J., & Gladden, L. F. (1998). FT-Raman studies of single-component and binary adsorption in silicalite-1. *Journal of the Chemical Society — Faraday Transactions*, *94*(8), 1157–1161.

Bakaev, V. A., & Steele, W. A. (1997). Hard rods on a line as a model for adsorption of gas mixtures on homogeneous and heterogeneous surfaces. *Langmuir*, *13*, 1054–1063.

Du, Z., Manos, G., Vlugt, T. J. H., & Smit, B. (1998). Molecular simulation of adsorption of short linear alkanes and their mixtures in silicalite. *A.I.Ch.E. Journal*, *44*(8), 1756–1764.

Dunne, J. A., Rao, M., Sircar, S., Gorte, R. J., & Myers, A. L. (1997). Calorimetric heats of adsorption and adsorption isotherms. 3. Mixtures of CH_4 and C_2H_6 in silicalite and mixtures of CO_2 and C_2H_6 in NaX. *Langmuir*, *13*, 4333–4341.

Guo, C. J., Talu, O., & Hayhurst, D. T. (1989). Phase transition and structural heterogeneity: Benzene adsorption on silicalite. *A.I.Ch.E. Journal*, *35*, 573–578.

Krishna, R. (1990). Multicomponent surface diffusion of adsorbed species. A description based on the generalized Maxwell–Stefan diffusion equations. *Chemical Engineering Science*, *45*, 1779–1791.

Krishna, R. (1993a). Problems and pitfalls in the use of the Fick formulation for intraparticle diffusion. *Chemical Engineering Science*, *48*, 845–861.

Krishna, R. (1993b). A unified approach to the modelling of intraparticle diffusion in adsorption processes. *Gas Separation and Purification*, *7*, 91–104.

Krishna, R., Smit, B., & Vlugt, T. J. H. (1998). Sorption-induced diffusion-selective separation of hydrocarbon isomers using silicalite. *Journal of Physical Chemistry A*, *102*, 7727–7730.

Krishna, R., Smit, B., & Vlugt, T. J. H. (1999). Influence of isotherm inflection on diffusion in silicalite. *Chemical Engineering Science*, *54*, 1751–1757.

Krishna, R., & Wesselingh, J. A. (1997). The Maxwell-Stefan approach to mass transfer. *Chemical Engineering Science*, *52*, 861–911.

Macedonia, M. D., & Maginn, E. J. (1999). Pure and binary component sorption equilibria of light hydrocarbons in the zeolite silicalite from grand canonical Monte Carlo simulations. *Fluid Phase Equilibrium*, *150–160*, 19–27.

Maurer, R. T. (1997). Multimodel approach to mixed-gas adsorption equilibria prediction. *A.I.Ch.E. Journal*, *43*(2), 388–397.

Micke, A., Bülow, M., Kocirik, M., & Struve, P. (1994). Sorbate immobilization in molecular sieves. Rate-limiting step for n-hexane uptake by silicalite-1. *Journal of Physical Chemistry*, *98*, 12337–12344.

Myers, A. L., & Prausnitz, J. M. (1965). Thermodynamics of mixed gas adsorption. *A.I.Ch.E. Journal*, *11*, 121–130.

O'Brien, J. A., & Myers, A. L. (1988). A comprehensive technique for equilibrium calculations in adsorbed mixtures: The generalized fast IAS method. *Industrial and Engineering Chemistry Research*, *27*, 2085–2092.

Rudzinski, W., Narkiewicz-Michalek, J., Szabelski, P., & Chiang, A. S. T. (1997). Adsorption of aromatics in zeolite ZSM-5: A thermodynamic-calorimetric study based on the model of adsorption and heterogeneous adsorption sites. *Langmuir*, *13*, 1095–1103.

Ruthven, D. M. (1984). *Principles of adsorption and adsorption processes*. New York: Wiley.

Shah, D. B., Guo, C. J., & Hayhurst, D. T. (1995). Intracrystalline diffusion of benzene in silicalite: Effect of structural heterogeneity. *Journal of the Chemical Society Faraday Transactions*, *91*, 1143–1146.

Sircar, S. (1991). Role of adsorbent heterogeneity on mixed gas-adsorption. *Industrial and Engineering Chemistry Research*, *30*(5), 1032–1039.

Sircar, S. (1995). Influence of adsorbate size and adsorbent heterogeneity on IAST. *A.I.Ch.E. Journal*, *41*(5), 1135–1145.

Smit, B. (1995). Simulating the adsorption isotherms of methane, ethane and propane in the zeolite silicalite. *Journal of Physical Chemistry*, *99*(15), 5597–5603.

Smit, B., & Maesen, T. L. M. (1995). Commensurate "freezing" of alkanes in the channels of a zeolite. *Nature*, *374*, 42–44.

Song, L., & Rees, L. V. C. (1997). Adsorption and transport of n-hexane in silicalite-1 by the frequency response technique. *Journal of the Chemical Society Faraday Transactions*, *93*, 649–657.

Sun, M. S., Shah, D. B., Xu, H. H., & Talu, O. (1998). Adsorption equilibria of C_1–C_4 alkanes, CO_2 and SF_6 on silicalite. *Journal of Physical Chemistry*, *102*, 1466–1473.

Sun, M. S., Talu, O., & Shah, D. B. (1996). Adsorption equilibria of C_5–C_{10} normal alkanes in silicalite crystals. *Journal of Physical Chemistry*, *100*, 17276–17280.

Takaishi, T., Tsutsumi, K., Chubachi, K., & Matsumoto, A. (1998). Adsorption induced phase transition of ZSM-5 by *p*-xylene. *Journal of the Chemical Society Faraday Transactions*, *94*, 601–608.

Van den Broeke, L. J. P., Bakker, W. J. W., Kapteijn, F., & Moulijn, J. A. (1999). Binary permeation through a silicalite-1 membrane. *A.I.Ch.E. Journal*, *45*, 976–985.

Van de Graaf, J. M., Kapteijn, F., & Moulijn, J. A. (1999). Modeling permeation of binary mixtures through zeolite membranes. *A.I.Ch.E. Journal*, *45*, 497–511.

Van de Graaf, J. M., Van der Bijl, E., Stol, A., Kapteijn, F., & Moulijn, J. A. (1998). Effect of operating conditions and membrane quality on separation performance of composite silicalite-1 membranes. *Industrial and Engineering Chemistry Research*, *37*, 4071–4083.

Vlugt, T. J. H., Krishna, R., & Smit, B. (1999). Molecular simulations of adsorption isotherms of linear and branched alkanes and their mixtures in silicalite. *Journal of Physical Chemistry B*, *103*, 1102–1118.

Vlugt, T. J. H., Zhu, W., Kapteijn, F., Moulijn, J. A., Smit, B., & Krishna, R. (1998). Adsorption of linear and branched alkanes in the zeolite silicalite-1. *Journal of the American Chemical Society*, *120*, 5599–5600.

Zhu, W., Graaf, J. M. v. d., Broeke, L. J. P. v. d., Kapteijn, F., & Moulijn, J. A. (1998). TEOM: a unique technique for measuring adsorption properties. Light alkanes in silicalite-1. *Industrial and Engineering Chemistry Research*, *37*(5), 1934–1942.